Breakup of Temperature Inversions in Deep Mountain Valleys: Part I. Observations

C. DAVID WHITEMAN

Pacific Northwest Laboratory, Richland, WA 99352

(Manuscript received 31 March 1981, in final form 7 December 1981)

ABSTRACT

The breakup of temperature inversions in the deep mountain valleys of western Colorado has been studied by means of tethered balloon observations of wind and temperature structure on clear weather days in different seasons. Vertical potential temperature structure profiles evolve following one of three patterns. Two of the patterns are special cases of the third pattern, in which inversions are destroyed by two continuous processes—upward growth of a convective boundary layer (CBL) into the base of the valley inversion, and descent of the inversion top. The three idealized patterns are described and 21 case studies of inversion breakup following the patterns are summarized. Inversion breakup begins at sunrise and is generally completed in 3½–5 h, unless the valley is snow covered or the ground is wet. Warming of the inversion layer is consistent with subsidence heating. An hypothesis is offered to explain the observations, stressing the role of the sensible heat flux in causing the CBL to grow and an upslope flow to develop over the sidewalls. As mass is removed from the base of the inversion layer in the upslope flows, the inversion sinks and warms.

1. Introduction

A number of investigators have commented on the lack of published observations of temperature structure evolution in the valley atmosphere (Geiger, 1965; Scorer, 1973; Reid, 1976). The importance of these observations in achieving a better understanding of local wind circulations and valley air pollution dispersion has become generally recognized in recent years, and has led to a recent research program investigating one aspect of the diurnally varying structure of the valley atmosphere, namely, the breaking or destruction of nocturnal temperature inversions. In Part I of this paper the design of the research program is presented, and data collected in the deep valleys of western Colorado are reviewed and analyzed. A general picture of the inversion destruction phenomenon is developed by induction and an hypothesis is developed to explain the observations. In Part II (Whiteman and McKee, 1982), a time-dependent thermodynamic model of vertical temperature structure is developed from the hypothesis to simulate vertical temperature structure evolution during inversion breakup. There, the model is tested against specific data sets to test its performance in situations where valley topography, initial inversion structure, and other external conditions vary.

2. Previous work

Ekhart (1949) published the first comprehensive set of frequent temperature profiles taken through the depth of a valley atmosphere during a clear day. The breakup of a 10°C, 1000 m deep nocturnal inversion occurred following sunrise and was accomplished by early afternoon. These initial observations had limited vertical resolution but clearly showed the development of a convective boundary layer (CBL) above the valley floor after sunrise and the apparent descent of a dry adiabatic layer into the valley from aloft. Machalek's (1974) observations on a clear spring day in Austria's deep Mürz Valley showed the dissipation of a nocturnal inversion (7°C in 500 m) in the hours between sunrise and noon, again accomplished by two processes, the heating of a boundary layer near the ground and the lowering of the upper boundary of the inversion. In view of the interesting initial observations of inversion breakup obtained by Ekhart and Machalek and the lack of a more comprehensive set of observations or understanding of the valley inversion breakup phenomenon, a set of experiments was designed to extend their work by collecting frequent concurrent wind and temperature profiles during the time of inversion destruction in mountain valleys of western Colorado.

3. Experimental design

The objective of the experimental program was to investigate the evolution of temperature inversion structure during undisturbed weather in a number of mountain valleys during different seasons, with the goal of elucidating the physical factors governing inversion destruction. To meet this objective, tethered balloon soundings of temperature and wind structure were to be made at approximately 1 h intervals during the time of inversion breakup, from

0021-8952/82/030270-20$09.00

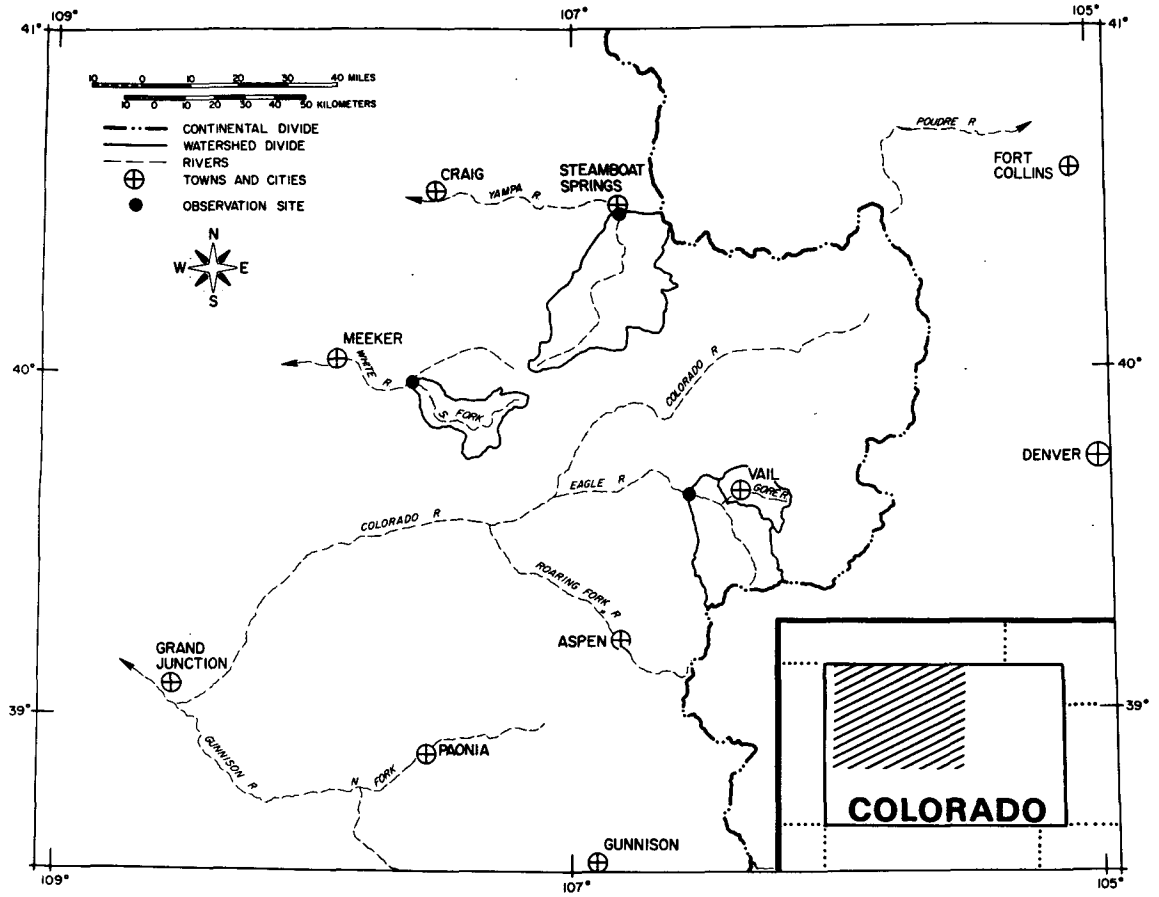

FIG. 1. Map of experimental areas showing valley watersheds. The lowest experimental site in each watershed is indicated by a dot.

sunrise to late morning. Experiments were designed to be conducted by a small number of people able to respond quickly to suitable synoptic weather patterns with a minimum amount of portable equipment.

Experiments were conducted primarily in valleys on the western slope of the Rocky Mountains in western Colorado (Fig. 1), where terrain elevations range from 1500 to nearly 4400 m MSL. Deep valleys having a simple linear shape and lack of topographic complexity were preferred to meet the experimental objective. Topographic characteristics of some of the valleys investigated are presented in Table 1. Further details concerning the determination of the numbers in the table, the other sites investigated, etc., are given by Whiteman (1980).

Small, portable, tethered balloon data collection systems (Morris *et al.*, 1975) provided the basic experimental data. A full description of these systems, tests of their operating characteristics, and a summary of data processing procedures are given by Whiteman (1980).

Following the experimental design, a basic data set of 375 tethered balloon soundings was obtained from Colorado valleys, representing inversion breakup observations in all seasons of the year. These data, collected primarily during undisturbed clear weather conditions, are representative of a rather narrow range of synoptic weather conditions in which high pressure generally prevailed over the experimental areas. These synoptic conditions occur frequently in western Colorado, especially in summer and fall.

4. General patterns of vertical potential temperature structure evolution

During inversion breakup in the valleys studied, the temperature structure evolved followed one of three patterns. These patterns, in an idealized form, are illustrated in Fig. 2. The first pattern of inversion destruction (Figs. 2a and 2b) is characterized by the upward growth from the ground of a convective boundary layer and describes inversion behavior over flat terrain. At sunrise (t_i) the potential temperature profile is as shown in Fig. 2a, and the height H of the CBL is zero (Fig. 2b). Successive soundings

TABLE 1. Topographic characteristics of experimental sites.

Valley site	Latitude	Longitude	Altitude (m MSL)	Height above valley floor (m)	Up-valley direction (°T)	Valley floor width (m)	Height of ridges above site (m)	Distance ridge to ridge (km)	Valley floor slope ($\times 10^{-3}$)	Slope aspect	Slope inclination (°)	Drainage area (km^2)	Nearest town
Yampa													
1. Sombrero ranch	40 27 27	106 48 50	2076	12	168	2580	450	5.5	2.6	E W	16 09	1370	Steamboat Springs
2. Horseshoeing school	40 27 00	106 48 49	2070	6	168	2580	450	5.5	2.6	E W	16 09	1370	
South Fork White River													
3. River cabin	39 58 26	107 37 29	2129	2	078	—	300	5.0	11.4	-	—	448	Buford
4. Mobley's Y-Z ranch	39 57 19	107 35 04	2175	2	128	400	350	3.0	10.0	N S	18 15	421	
5. Stillwater	39 55 03	107 32 43	2295	12	157	850	750	7.8	0.5	E W	12 12	405	
Eagle													
6. Steve Miller residence	39 38 23	106 34 33	2222	12	104	1450	700	9.2	7.0	N S	21 10	1061	Edwards
7. Ray Miller ranch	39 38 28	106 34 20	2228	18	104	1450	700	9.2	7.0	N S	21 10	1061	
8. Slope site 1	39 39 53	106 34 14	2530	320	104	1450	400	9.2	7.0	N S	21 10	1061	
9. Slope site 2	39 39 54	106 34 15	2533	323	104	1450	400	9.2	7.0	N S	21 10	1061	
Gore													
10. Vail Safeway	39 37 50	105 25 06	2426	15	046	390	600	3.8	17.4	NW SE	14 24	233	Vail
11. Vail municipal building	39 38 37	106 22 48	2493	15	093	530	700	5.1	13.4	N S	15 16	180	
12. Vail golf course	39 38 34	106 20 37	2518	10	077	320	650	3.0	9.4	N S	26 25	152	

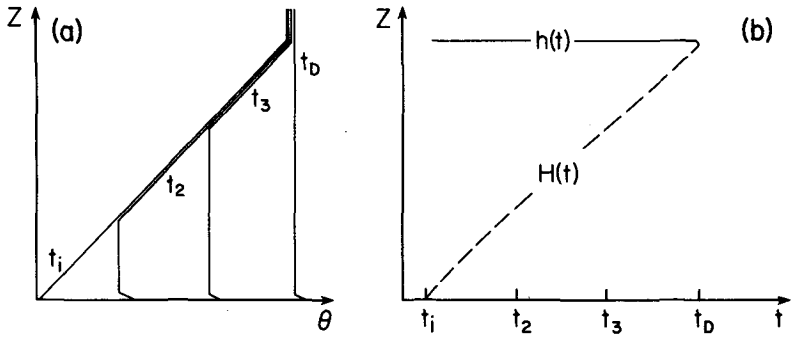

Pattern 1. Growth of CBL.

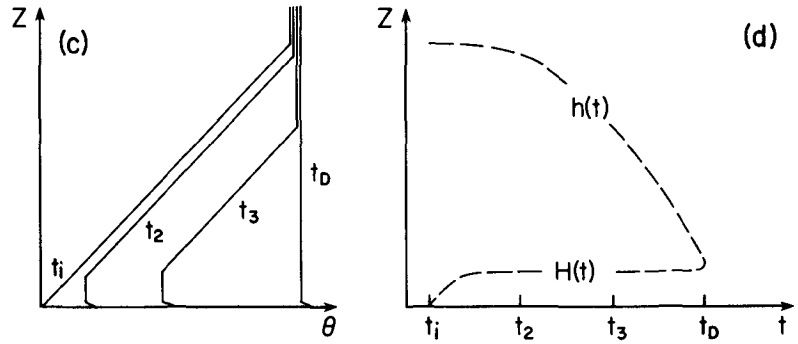

Pattern 2. Descent of inversion top and arrested growth of CBL.

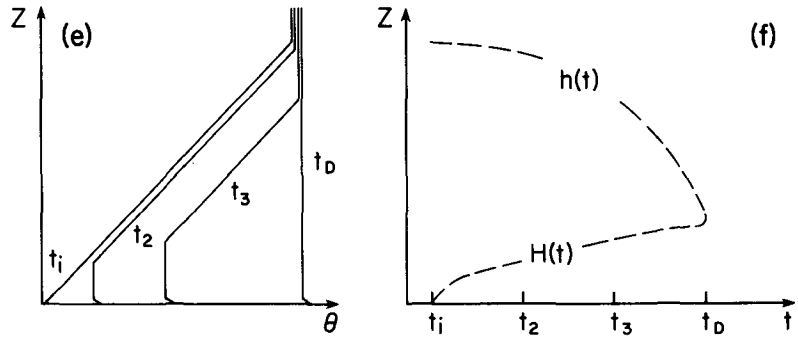

Pattern 3. Descent of inversion top and continuous growth of CBL.

FIG. 2. Three patterns of temperature structure evolution. Potential temperature profiles are on the left and time-height analyses of CBL height and inversion top height are on the right.

taken at times t_2 and t_3 show the upward growth from the ground of a well-mixed convective boundary layer. At any given time the boundary layer has a potential temperature that is nearly independent of height, but the temperature of the boundary layer increases as a function of time. A shallow superadiabatic sublayer is typically present at the base of the CBL immediately above the ground. The inversion is finally destroyed at time t_D when the height $H(t)$ of the CBL grows to the height h of the top of the inversion, producing a constant potential temperature atmosphere in the valley. Pattern 1 inversion destruction is thus characterized by the growth with time of a convective boundary layer, while the height of the top of the inversion remains fixed in time. Only one example of Pattern 1 inversion destruction was observed in the field experiments. This occurred on a summer day in the widest valley studied.

The second pattern of temperature structure evo-

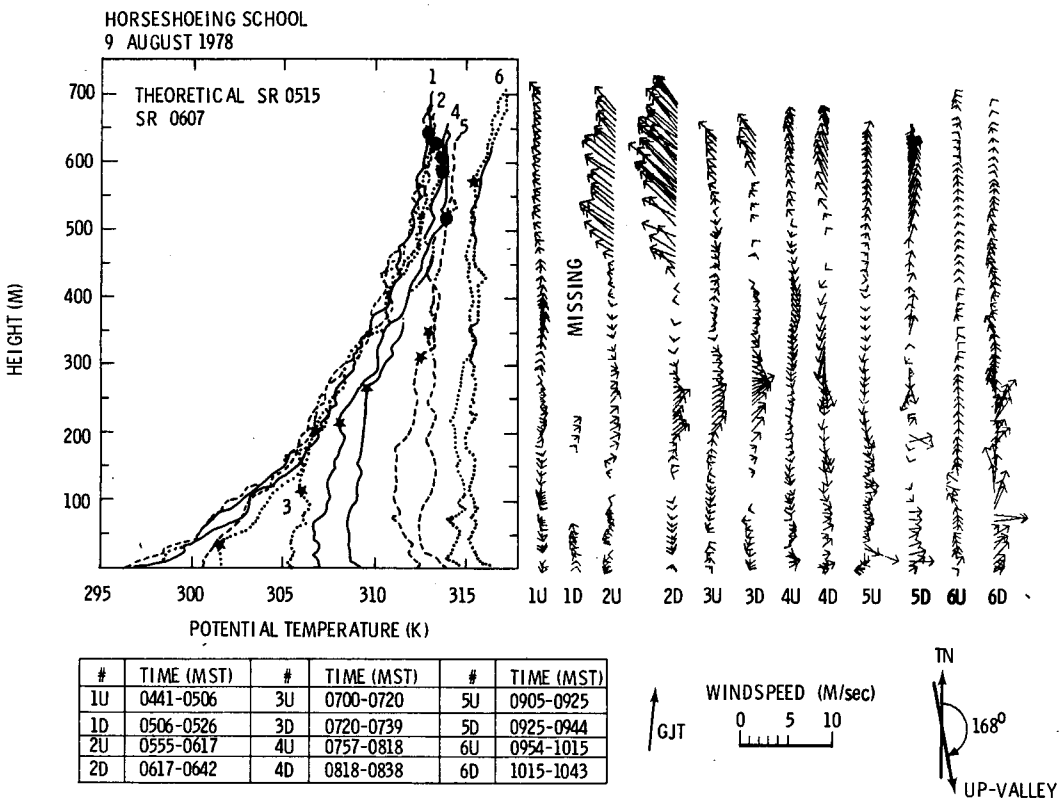

#	TIME (MST)	#	TIME (MST)	#	TIME (MST)
1U	0441-0506	3U	0700-0720	5U	0905-0925
1D	0506-0526	3D	0720-0739	5D	0925-0944
2U	0555-0617	4U	0757-0818	6U	0954-1015
2D	0617-0642	4D	0818-0838	6D	1015-1043

FIG. 3. Example of Pattern 1 temperature structure evolution. Tethered-balloon data, Yampa Valley, 9 August 1978.

lution is very different from the first. The CBL over the valley floor, which begins to grow after sunlight illuminates the valley floor, plays only a minor role, its growth being arrested after a certain shallow height is attained (Fig. 2d). The inversion destruction is caused by the descent of the top of the inversion into the valley, which is accompanied by a warming of the valley atmosphere (Fig. 2c). Despite this warming, the vertical potential temperature gradient in the inversion layer remains constant. The inversion is destroyed at time t_D when the descending top of the inversion meets the fixed top of the CBL and the warming finally results in an equal potential temperature throughout the valley depth. This pattern of inversion destruction was observed twice during field experiments. Both cases occurred in winter when the valleys had extensive snow cover.

Pattern 3 temperature structure evolution is a combination of the first and second patterns. In Pattern 1, a CBL grows upward into the inversion and the descent of the top of the inversion plays no role. In Pattern 2, inversion destruction is accomplished by a descending inversion top, and the role of the CBL is minimized. Pattern 3 represents a continuum of intermediate situations in which both the growth of the CBL and the descent of the inversion top are present. Figs. 2e and 2f show the continuous growth of the height $H(t)$ of the CBL and the accompanying descent of the inversion top, $h(t)$. The elevated remnant of the temperature inversion warms significantly but maintains its original potential temperature gradient. The inversion is finally destroyed at time t_D when the descending inversion top meets the ascending CBL, and a constant potential temperature is attained through the depth of the valley. Pattern 3 inversion destruction is the most common pattern in Colorado valleys. It was observed in all seasons, provided snow cover was absent, and its occurrence seemed to be largely independent of topography, synoptic conditions and upper level winds. Of 21 case studies selected for further analysis, 18 followed Pattern 3.

The three patterns of inversion destruction differ in the extent to which the CBL growth or inversion top descent is dominant. Three main layers of temperature structure may be recognized in the idealized vertical profiles—the CBL, the elevated inversion, and the neutral layer above the inversion. Following are examples taken from the data illustrating the three patterns of potential temperature structure evolution.

An example of Pattern 1 inversion destruction was observed on the morning of 9 August 1978 in the Yampa Valley, 3 km upstream from Steamboat Springs, Colorado. The data are given in Fig. 3. The table at the base of the figure gives the tethersonde

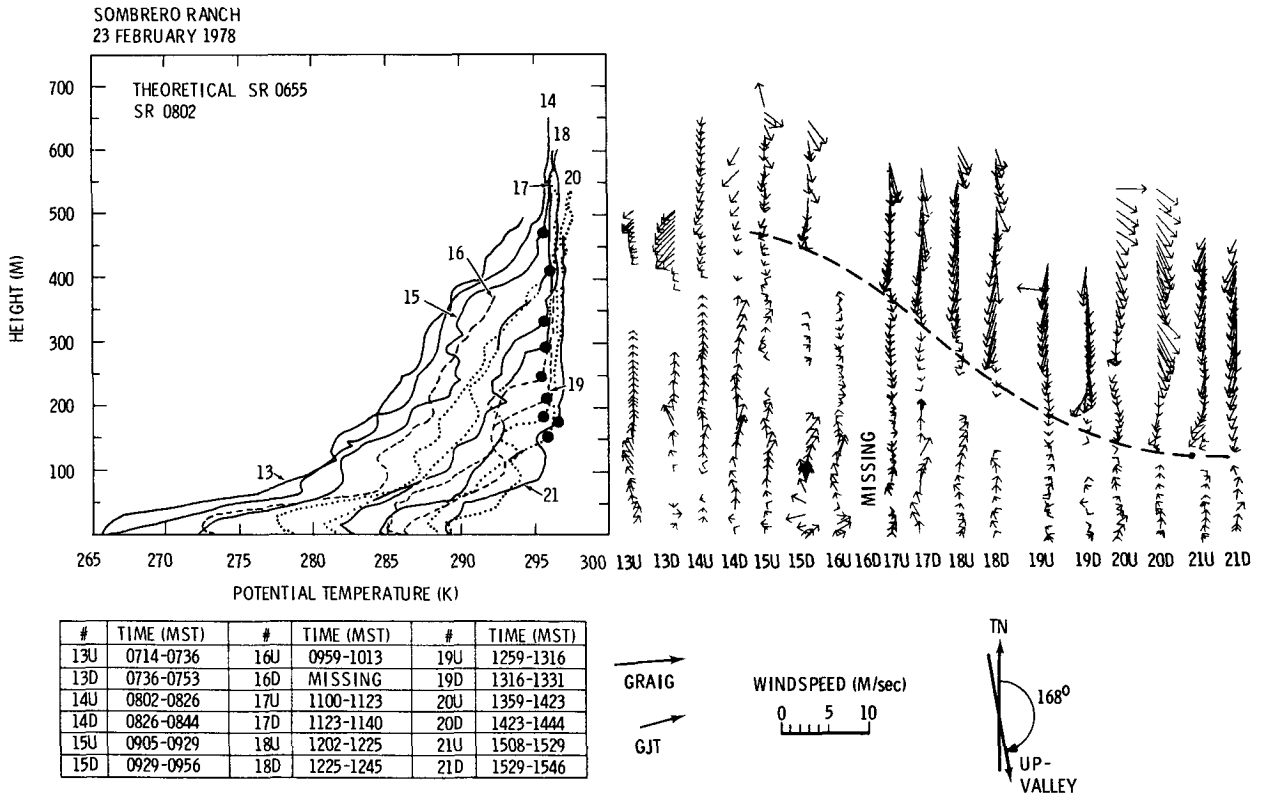

#	TIME (MST)	#	TIME (MST)	#	TIME (MST)
13U	0714-0736	16U	0959-1013	19U	1259-1316
13D	0736-0753	16D	MISSING	19D	1316-1331
14U	0802-0826	17U	1100-1123	20U	1359-1423
14D	0826-0844	17D	1123-1140	20D	1423-1444
15U	0905-0929	18U	1202-1225	21U	1508-1529
15D	0929-0956	18D	1225-1245	21D	1529-1546

FIG. 4. Example of Pattern 2 temperature-structure evolution. Tethered-balloon data, Yampa Valley, 23 February 1978.

sounding number (U for an up-sounding, D for a down-sounding) and the time interval in which the sounding was conducted. Plots of potential temperature versus height form the main part of the figure and concurrent soundings of vertical wind structure, labeled with the sounding number, are located adjacent to the potential temperature plots. The orientation of the wind arrows at a particular height in the soundings can be compared to the up-valley direction provided on the figure. A wind speed legend is given so that the length of the wind arrows can be converted to actual wind speeds. The 0415 MST 700 mb Grand Junction vector wind is given for reference. The time of sunrise (theoretical SR) on an unshaded horizontal surface at the latitude and longitude of the experimental site is indicated, along with the time of actual sunrise (SR) at the valley floor site. The heights of the inversion top and CBL top are indicated by dots and stars, respectively, on the individual soundings. The primary means of making these subjective height estimates was to find the inflection points between potential temperature gradients in the three main temperature structure layers. In difficult cases, continuity of trends in the heights of the various layers was invoked. In some cases wind discontinuities at the boundaries of the layers helped in the analysis.

The basic features of the Pattern 1 inversion destruction are seen in the Yampa Valley data presented in Fig. 3. The first sounding of the morning was taken before sunrise and reveals the hyperbola-shaped vertical profile of a 650 m deep inversion with a strength of 16 K. Successive profiles show the development of a convective boundary layer that grows upward from the surface. Major warming occurs only in the CBL. The inversion destruction did not follow Pattern 1 perfectly, but showed some of the characteristics of Pattern 3 destruction as observed in most other valleys, including some warming of the inversion layer and an apparent, but minor, descent of the top of the inversion. Winds within the inversion were very weak and erratic during the inversion destruction except at the upper levels where southeast winds of 4 or 5 m s^{-1} prevailed for a time. Up-valley and up-slope winds tended to form in the CBL as it grew upwards from the ground. After inversion destruction (sounding 5D), weak down-valley winds prevailed through the depth of the valley.

Pattern 2 inversion destruction was observed in the snow-covered Yampa Valley on 23 February 1978 and in the Gore Valley on 10 December 1975. The 23 February 1978 data (Fig. 4) are a particularly good example of Pattern 2 destruction. The first soundings of the morning show an intense potential temperature inversion of 30 K in 500 m. The inversion had a hyperbolic shape in the lowest level that resulted in a particularly intense potential temperature gradient of 183 K km^{-1} in the lowest 73 m of

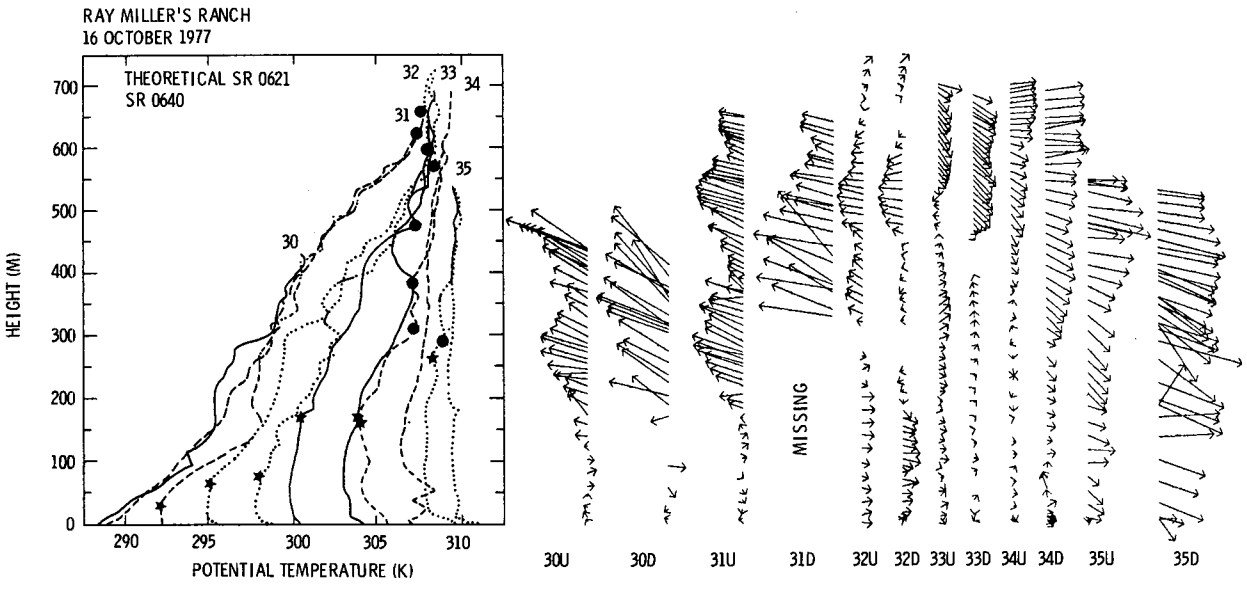

#	TIME (MST)	#	TIME (MST)	#	TIME (MST)
30U	0559-0617	32U	0829-0848	34U	1013-1033
30D	0617-0630	32D	0848-0913	34D	1033-1055
31U	0650-0719	33U	0924-0948	35U	1106-1121
31D	0719-0738	33D	0948-1011	35D	1121-1138

FIG. 5. Example of Pattern 3 temperature-structure evolution. Tethered-balloon data, Eagle Valley, 16 October 1977.

the profile. The hyperbolic segment of the profile was surmounted by a near-linear segment having many small potential temperature deformations. A fairly sharp discontinuity at the top of the linear segment marked the beginning of isothermal to neutral stability. The soundings were of insufficient depth to resolve the upper limit of this layer. Successive soundings show the inversion structure evolving according to Pattern 2. The descent of the inversion top began after sounding 14 and is clearly seen in the data. By 0959 MST a shallow boundary layer, comprised mostly of a superadiabatic sublayer with only a shallow layer of constant potential temperature, had grown upward from the ground. After reaching a height of ~35 m, the boundary layer failed to grow further. Inversion destruction thereafter was accomplished entirely by the descent of the inversion top. During the descent, temperatures within the inversion layer warmed at about the same rate at all levels. The potential temperature θ_h at the top of the inversion warmed 1–1.5 K during the day as the inversion destruction progressed. By late in the afternoon, the inversion had not been completely destroyed, although the top of the inversion had descended to within 175 m of the ground. Further soundings (22 on) showed the reestablishment of the nocturnal cooling regime and the end of the inversion destruction period.

Winds within the inversion during the Pattern 2 destruction blew predominantly down the valley, but at speeds generally less than 2 m s^{-1}. Winds in the neutral layer above the inversion blew up the valley at speeds of several meters per second. The approximate boundary between the two wind regimes is shown in the figure.

A Pattern 3 inversion destruction occurred in the Eagle Valley on 16 October 1977 (Fig. 5). Although the first sounding of the morning was terminated at an altitude of only 450 m, it is apparent from the second sounding that the near-sunrise inversion extended to a height of ~650 m and had a strength of ~19.5 K. The average potential temperature gradient was 30 K km^{-1}. The initial inversion shape was nearly linear, and the potential temperature evolution followed Pattern 3 very closely. The ascent of the CBL and the descent of the top of the inversion are well marked, as is the strong warming at mid-levels of the profiles. During the period of inversion destruction, the elevated remnants of the near-sunrise inversion maintained their potential temperature gradient, and the neutral layer warmed by 1.5 K. The inversion had been completely destroyed by the last down-sounding at ~1130 MST.

Along-valley wind systems are particularly well developed in the Eagle Valley. Strong down-valley winds usually begin in the early evening and persist through the night, as evidenced by the strong down-valley winds at mid-levels in the inversion in the early

morning soundings. Winds within the elevated inversion layer often continue to blow down-valley until the inversion is nearly broken, but usually weaken slowly as the inversion descends. In the CBL below, the winds are typically weak and blow up-valley. Up-valley winds in the neutral layer above the inversion often follow the descent of the inversion top deeper and deeper into the valley until, when the inversion is broken, they prevail throughout the whole depth of the valley. At this time they often become more turbulent. The neutral layer wind strengths as well as those of the inversion layer and CBL, are quite variable from day to day and from valley to valley and are considerably more variable than the temperature structure patterns previously described. In the following section, additional case studies of inversion breakup will be summarized.

5. Vertical temperature structure evolution data—21 case studies

Twenty-one case studies of inversion destruction illustrate the range of seasonal, topographic and synoptic conditions for which the previously described inversion evolution patterns were observed. The data were collected at nine sites in four Colorado valleys. Most case studies were conducted on days with a 500 mb ridge and a surface high pressure area over the western United States. However, there were a significant number of days on which weather disturbances were present in the experimental areas. See Whiteman (1980) for further details. Nevertheless most days chosen for analysis were characterized by a lack of significant cloud cover. Wind speeds at 700 mb were consistently light on experimental days, averaging just over 6 m s^{-1}, although winds were from all quadrants. Wind speeds at 500 mb averaged 10.8 m s^{-1}, but varied from 1 to 28 m s^{-1} with winds consistently from the two western quadrants.

Inversion destruction data for the 21 case studies are summarized in Table 2. Several comments on the table are necessary:

- t_i, the time of theoretical sunrise for the latitude and longitude of the site, is entered in column 3.
- t_i', the time at which direct sunlight first reached the observational site on the valley floor, is entered in column 4 as recorded from field notes.
- t_D, an estimate of the time of final destruction of the inversion, is entered in column 5. These time estimates were based on the series of temperature profiles taken during inversion destruction and indicate the time at which the entire valley depth would attain a constant potential temperature.
- h_i, the initial depth of the inversion, is recorded in column 7.
- h_v, the valley depth, is given in column 8.
- Inversion strength, the potential temperature difference between the base of the sounding and the top of the inversion, is given in column 10.
- γ, the average potential temperature gradient recorded on the first sounding of the morning, is given in column 11.
- γ', the average potential temperature gradient within the inversion layer at a time approximately midway through the inversion destruction period, is given in column 12.
- $\Delta\theta_h$, the increase in potential temperature of the neutral layer above the valley inversion during the period of inversion destruction, shown in column 6, is given in column 13.
- The peak strength (m s^{-1}) of the down-valley wind within the inversion at a time near sunrise is given in column 14. The value given is an average of the wind speeds recorded by the up- and down-soundings at the altitude of the peak down-valley wind. This averaging was necessary to account for systematic differences between the winds indicated by up- and down-soundings, as discussed by Whiteman (1980).

a. Inversion characteristics near the time of sunrise

For the 21 case studies, the average depth of the valley inversions was 604 m (Table 2, column 7). Inversion depths ranged from 400 m at the Stillwater site to 750 m in the Gore Valley. In undisturbed clear weather, inversions at a particular site attain a depth typical of the site, regardless of season. Thus for the Eagle Valley sites, which are close together, inversions typically grow to about 625 m. Inversions at the two valley sites in the Yampa Valley, which again are not far apart, are 475–650 m deep. Inversions at the Stillwater site on the South Fork of the White River, investigated in only one season, attain heights of only 300 or 400 m.

For the valleys studied, inversions generally built to the level of the ridgetops (Table 2, columns 8 and 9). The average ratio of inversion depth to valley depth was 1.10, although the ratio varied from 0.53 at the Stillwater site to 1.75 at the River Cabin. While the average inversion top height is slightly above the level of the local ridgetops, the height of the inversion top in all cases is lower than the height of regional terrain features in the vicinity of the sites.

Inversion strength (Table 2, column 10) averaged 17.1 K for the cases studied and varied from 10.7 K for a shallow summer inversion in the South Fork of the White Valley to 30.0 K for a moderately deep inversion under clear skies in the snow-covered Yampa Valley. The primary factors affecting inversion strength appear to be cloudiness, which decreases inversion strength, and snow cover on the ground, which increases it. Snow cover was present during two campaigns. In February 1978, the Yampa Valley was covered with a deep snowpack. In De-

TABLE 2. Summary of inversion breakup data.

(1) Location	(2) Date	(3) t_t (MST)	(4) t'_i (MST)	(5) t_D (MST)	(6) $t_D - t_t$ (h min)	(7) h_t (m)	(8) h_e (m)	(9) $\frac{h_t}{h_e}$	(10) Inversion strength (K)	(11) ($K^2 m^{-1}$)	(12) ($K^2 m^{-1}$)	(13) $\Delta\theta_h$ (K)	(14) Valley Wind System Strength (m sec^{-1})	(15) Clouds	(16) Comments
Yampa Valley															
1. Sombrero	02-23-78	0655	0802	—	—	530	450	1.18	30.0	0.0566	0.0345	1.1	2.1	Clear	Snow Cover
2. Horseshoe	08-09-78	0515	0607	0945	4:30	650	450	1.44	16.0	0.0246	0.0187	1.5	1.7	Clear	
3. Horseshoe	08-10-78	0516	0608	1000	4:44	535	450	1.19	17.5	0.0327	0.0256	1.3	1.4	0.1 → 0.5Cu	Thunderstorm distant N and S.
South Fork White Valley															
4. River cabin	08-26-78	0535	0606	0930	3:55	525	300	1.75	14.1	0.0269	0.0208	2.5	6.8	0.7Cu → CLR → 0.1Cu	
5. Stillwater	08-27-78	0536	0710	1030	4:54	400	750	0.53	10.7	0.0268	0.0160	1.5	10.0+	Clear	
6. Mobley	08-27-78	0536	0643	0920	3:44	600	350	1.71	20.0	0.0333	0.0250	0.4	9.8	Clear	
7. Mobley	08-29-78	0538	0644	1010	4:32	530	350	1.51	19.5	0.0368	0.0280	2.1	9.3	Clear	
8. River cabin	08-29-78	0538	0619	1035	4:57	525	300	1.75	17.8	0.0339	0.0154	1.5	7.5	Clear	
Eagle Valley															
9. Ray Miller	10-13-77	0618	0637	1130	5:12	675	700	0.96	17.9	0.0265	0.0288	3.8	7.5	Clear	
10. Ray Miller	10-14-77	0619	0638	1110	4:51	625	700	0.89	15.6	0.0250	0.0222	3.5	5.8	0.2 → 0.6 → 0.2Ci	
11. Ray Miller	10-16-77	0621	0640	1130	5:09	650	700	0.93	19.5	0.0300	0.0269	1.5	7.5	Clear	
12. Steve Miller	04-20-78	0527	0545	0945	4:18	625	700	0.89	11.7	0.0187	0.0182	4.2	3.5	CLR → 0.8-Ci	
13. Steve Miller	07-08-78	0450	0523	0910	4:20	575	700	0.82	19.3	0.0336	0.0280	1.1	2.3	Clear	
14. Steve Miller	07-09-78	0451	0524	0940	4:29	620	700	0.89	16.0	0.0337	0.0238	1.0	6.8	CLR → sctd Ac	
15. Steve Miller	10-11-78	0616	0703	1030	4:14	725	700	1.04	16.3	0.0225	0.0192	2.3	4.5	sctd Ci → CLR	Sun obscured by clouds near sunrise
16. Steve Miller	10-12-78	0617	0646	1015	3:58	585	700	0.84	15.3	0.0262	0.0200	2.3	4.0	Clear	
17. Steve Miller	10-19-78	0623	0642	1245	6:22	700	700	1.00	15.4	0.0220	0.0200	5.5	7.5	Clear	Rain yesterday
Gore Valley															
18. Safeway	12-10-75	0720	0900	1200	4:40	525	600	0.88	17.0	0.0378	0.0290	0.0	0.5	Clear	1st sndng 0830, h_t estimated, snow cover.
19. Municipal bldg.	10-19-77	0623	0714	1030	4:07	585	700	0.84	16.0	0.0274	0.0216	2.0	4.0	Clear	
20. Municipal bldg.	07-06-78	0448	0558	0930	4:42	750	700	1.07	17.5	0.0233	0.0211	0.9	3.6	Clear	
21. Municipal bldg.	07-07-78	0449	0558	0845	3:56	750	700	1.07	15.2	0.0203	0.0224	2.1	6.3	Clear	
Mean					4:35	604	590	1.10	17.1	0.0295	0.0231	2.0	5.4		

cember 1975, the Gore Valley had a cover of snow on the forested north-facing hillside but had only patchy snow cover on the south-facing hillside. Inversion depth has only a limited effect on inversion strength, with deep inversions being relatively weaker than shallow inversions, other things being equal.

The potential temperature gradient at a particular site (Table 2, column 11), being a ratio of inversion strength and inversion depth, will be controlled by cloudiness and/or snow cover. The average potential temperature gradient for the valleys investigated was 0.0295 K m^{-1}, but values ranged from 0.0187 to 0.0566 K m^{-1}. The average potential temperature gradient, defined as the difference in potential temperature between the top of the inversion and the surface divided by inversion depth, is often not representative of the potential temperature gradient at mid or upper levels of the inversion. This is especially apparent when a shallow intense inversion sublayer is present at the base of the inversion. A second calculation of potential temperature gradient for mid and upper levels of the inversion is given in column 12 of Table 2 for a time approximately mid-way through the inversion destruction period. The average of this figure for the 21 case studies is 0.0231 K m^{-1}.

Near-sunrise soundings of potential temperature frequently showed an especially strong temperature inversion in the lowest layers of the profiles. These segments of the profiles were often of a hyperbolic shape, especially apparent in valleys that were snow-covered, in which down-valley winds were light or in which a terrain constriction down-valley caused local pooling of cold air. In valleys that supported a moderate or strong down-valley wind system, on the other hand, the vertical profiles of potential temperature were near-linear through the depth of the inversion. Peak down-valley winds (Table 4, column 14) within the inversions of some valleys were in the range from 8 to 11 m s^{-1}. Inversions were not destroyed by these strong winds, nor were the gross inversion characteristics significantly affected, except for the above-mentioned effect of the linearization of the inversion profiles.

Seasonal differences in the characteristics of valley inversions are not large. As mentioned above, inversion strength is increased by snow cover. There also seems to be a tendency for summer inversions to be slightly deeper, but not stronger. This is more clearly seen in the Yampa and Gore Valley data.

It is of interest to compare the characteristics of western Colorado valley inversions with the characteristics of inversions on the same dates at Grand Junction, Colorado, the nearest National Weather Service rawinsonde site. The Grand Junction site is at an altitude of 1475 m MSL on the broad Colorado River west of the study region. Morning rawinsondes there are generally launched at 0415 MST, before sunrise in all seasons. Data in Table 3 include temperature inversion characteristics as well as 700 and 500 mb wind speeds and directions, as obtained from Grand Junction rawinsondes.

For most of the valley sites, the 700 mb level is just above ridgetops. The 500 mb level is at least 1000 m above the crest of the Rocky Mountains. Columns 6, 7, 9 and 10 of Table 3 give the along-valley and cross-valley components of the Grand Junction winds for the specified valley site. A positive number for the along-valley component indicates an up-valley flow. A positive number for the cross-valley component indicates a flow from right to left when looking up the valley.

Inversions at Grand Junction are usually much shallower than the valley inversions, averaging only 198 m deep, but varying from 49 to 349 m. Inversion strengths at Grand Junction range from 2.6 to 11.5 K, but average 6.7 K, versus 17.1 K for the valley inversions. The potential temperature gradient of Grand Junction inversions, averaging 0.0409 K m^{-1} with a range of 0.0152 to 0.0797 K m^{-1}, is considerably stronger than for the valley inversions. All inversion characteristics at Grand Junction are significantly more variable than the characteristics of the deep valley inversions studied.

Due to the selection of meteorologically undisturbed experimental periods, valley inversion data were generally collected when 700 and 500 mb wind speeds were low. The effect of upper winds on the development of valley inversions and Grand Junction inversions can be seen by comparing data in Tables 2 and 3. The Eagle Valley data suggest that strong 700 mb cross-valley winds may result in slightly shallower inversions than normal. But, at least for the range of wind speeds studied, no obvious and consistent relationship between upper air winds and valley temperature inversion development can be determined, even when the upper level winds are resolved into along- and cross-valley components.

b. Inversion breakup

Data indicate that inversion destruction typically begins shortly after sunrise (t_i) with the beginning of the descent of the top of the inversion. The growth of the convective boundary layer on the valley floor is initiated after direct sunlight arrives at the floor. Depending on the valley topography and orientation, local sunrise (t_i') may be up to 1 h and 50 min later than t_i (Table 2, columns 3 and 4). A developing boundary layer was usually readily apparent in temperature soundings within 30–40 min after sunlight reached the valley floor.

The amount of time after sunrise required for an inversion to be destroyed varies from 3½ to 5 h. These are rather narrow limits, considering the wide variation in topography and broad seasonal sampling of

TABLE 3. Grand Junction 0415 MST rawinsonde data corresponding to valley data of Table 2.

(1) Date	(2) Inversion depth (m)	(3) Inversion strength (K)	(4) (3)/(2) (K m^{-1})	(5) 700 mb wind (deg/m s^{-1})	(6) Along-valley component (m s^{-1})	(7) Cross-valley component (m s^{-1})	(8) 500 mb wind (deg/m s^{-1})	(9) Along-valley component (m s^{-1})	(10) Cross-valley component (m s^{-1})
Yampa									
1. 02-23-78	306	6.7	0.0219	255/05	−0.26	4.99	275/09	2.63	8.61
2. 08-09-78	49	2.6	0.0531	185/07	−6.69	2.05	320/08	7.06	3.76
3. 08-10-78	349	5.3	0.0512	255/07	−0.37	6.99	310/10	7.88	6.16
South Fork White River									
4. 08-26-78	202	6.3	0.0312	245/06	5.85	1.35	230/08	7.06	3.76
5. 08-27-78	270	11.2	0.0415	275/04	1.88	3.53	255/09	1.25	8.91
6. 08-27-78	270	11.2	0.0415	275/04	3.35	2.18	255/09	5.42	7.19
7. 08-29-78	79	6.3	0.0797	300/02	1.49	−1.34	255/08	7.99	0.42
8. 08-29-78	79	6.3	0.0797	300/02	1.98	0.28	255/08	4.81	6.39
Eagle									
9. 10-13-77	192	3.3	0.0172	230/05	2.94	4.05	210/07	1.93	6.73
10. 10-14-77	172	5.3	0.0308	040/07	−3.07	6.29	340/06	3.36	−4.97
11. 10-16-77	140	7.1	0.0507	235/06	3.94	4.53	220/07	3.07	6.29
12. 04-20-78	88	5.7	0.0648	255/06	5.25	2.91	270/10	9.70	2.42
13. 07-08-78	196	8.5	0.0434	255/14	12.24	6.79	225/23	11.85	19.71
14. 07-09-78	266	4.6	0.0173	250/08	6.63	4.47	235/12	7.87	9.06
15. 10-11-78	278	5.0	0.0180	290/03	2.98	−0.31	335/11	6.92	−8.55
16. 10-12-78	159	11.5	0.0723	325/06	4.53	−3.94	320/13	10.52	−7.60
17. 10-19-78	256	8.5	0.0332	235/05	3.28	3.77	255/10	8.75	4.85
Gore									
18. 12-10-75	315	10.3	0.0327	230/10	9.98	−0.70	260/18	14.92	−10.07
19. 10-19-77	176	6.7	0.0381	250/06	5.52	2.34	205/11	4.12	10.20
20. 07-06-78	—	—	—	260/02	1.95	0.45	255/11	10.46	3.40
21. 07-07-78	79	5.9	0.0747	175/02	−0.28	1.98	260/15	14.62	3.37
Mean	198	6.7	0.0409						
Minimum	49	2.6	0.0152						
Maximum	349	11.5	0.0797						

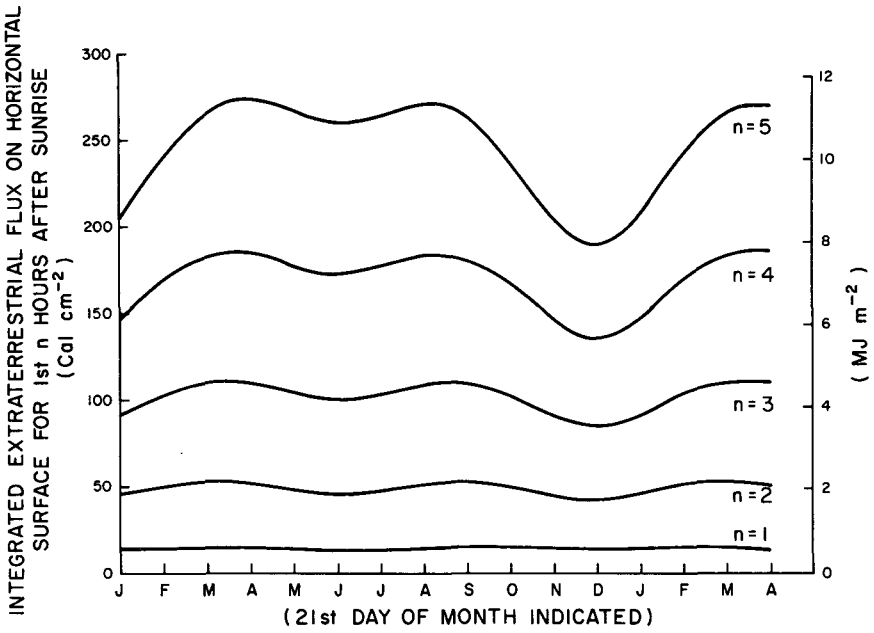

FIG. 6. Time-integrated solar flux on an extraterrestrial horizontal surface as a function of month of year for the first *n* hours following sunrise. For latitude and longitude of Steamboat Springs, Colorado.

data. For 20 cases listed in Table 2, the average time required for destruction was 4 h and 35 min. An exception was the inversion of 23 February 1978 in the snow-covered Yampa Valley, since it was maintained all day, even though it underwent a clear evolutionary cycle. The 19 October 1978 inversion in the Eagle Valley also took an unusually long time to be destroyed. This is probably due to the fact that rain had fallen in the valley on the previous day. The small range in the time required to break the inversions may seem to be a curious result. After all, energy is required to break inversions, and one would perhaps expect inversions to break more rapidly in the summertime than in the winter when insolation is weak. However, application of a standard radiation model (Sellers, 1965) shows that the integrated (extraterrestrial) solar flux on a horizontal surface at the latitude of the experimental areas for the first 3½–5 h after sunrise varies only slightly with season, except for a brief period around the winter solstice (Fig. 6).

The rates of descent of the inversion top and ascent of the CBL for a subset of the 21 case studies are seen in Fig. 7 where the heights of these features are plotted against time. The tops of the inversions descend after sunrise in all of the cases studied, as specified for Pattern 2 and 3 temperature structure evolution. The rate of descent usually increases with time, but in a few of the case studies, the inversion descent rate remains nearly constant during much of the inversion destruction period. This constant rate of descent, previously described by Whiteman and McKee (1977), is particularly marked for the 10 December 1975 inversion destruction in the Gore Valley. Inversion descent in one of the case studies was unusual. In the Yampa Valley on 9 August 1978, the single example approximating Pattern 1 inversion destruction observed in the experiments, the descent of the inversion top was arrested ~4 h after sunrise when the inversion top began to ascend. The main feature of the inversion destruction on this day is the growth of the CBL. From Table 2, most inversions are broken in ~4½ h, and the average inversion is 604 m deep initially. Since the inversion is broken when the descending inversion top meets the ascending CBL at ~250 m above the valley floor, the average rate of inversion descent is (604 − 250 m)/4.5 h = 79 m h^{-1}. The observed ascent of the CBL from the valley floor typically begins ~1 h after sunrise. The rate of growth of the CBL over the valley floor varies from site to site and from case to case, but the average rate of ascent is ~250 m/3.5 h = 71 m h^{-1}. The CBL grows quickly initially, but then the rate of growth usually decreases. This tendency for a decrease in growth rate often occurs when the CBL reaches a depth of ~50 m. The rate of CBL ascent and inversion top descent increase significantly just before the final destruction of the inversion. This may be due to a sudden breakup or overturning of the shallow remnants of the elevated inversion layer. The course of the two curves, constructed from intermittent balloon soundings, is usu-

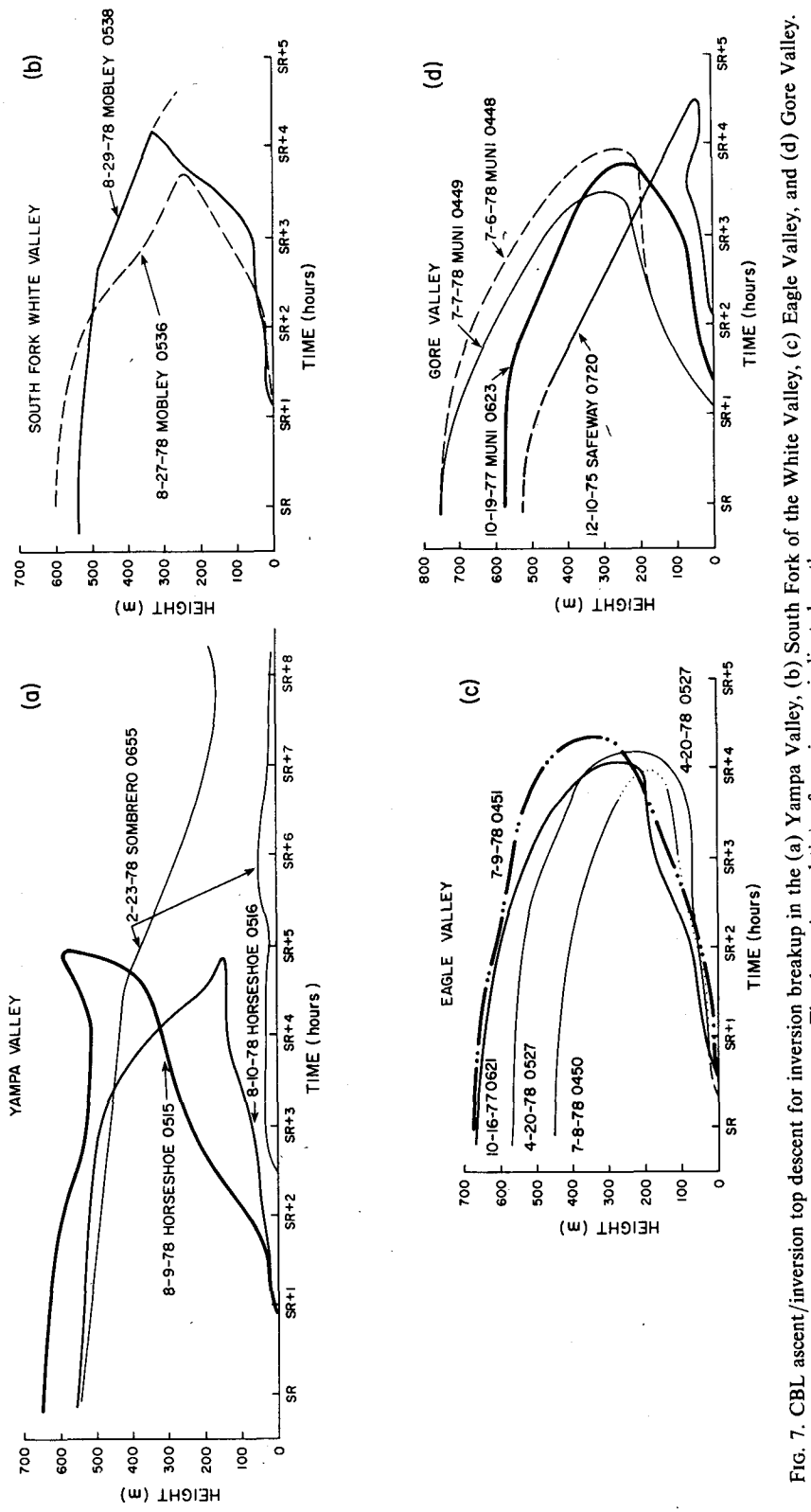

FIG. 7. CBL ascent/inversion top descent for inversion breakup in the (a) Yampa Valley, (b) South Fork of the White Valley, (c) Eagle Valley, and (d) Gore Valley. The data, site and time of sunrise are indicated on the curves.

ally ill-defined at this critical point, since final destruction may take place abruptly.

Those familiar with the literature on mountain and valley wind systems will note the resemblance between Fig. 7 and Davidson and Rao's (1963) Fig. 9. Davidson and Rao's figure, derived from pilot balloon observations of valley wind structure, showed the descent of a boundary in the wind structure corresponding in time and position to the inversion top plotted in Fig. 7. Their boundary separated the down-valley winds that prevailed within the valley, from the winds aloft. The correspondence should not be surprising since our observations show that winds usually reverse, or at least shift direction at the top of a valley inversion. Other aspects of the wind structure during inversion breakup proved interesting and will be discussed in the next section.

6. Wind structure evolution during inversion breakup

Case study data presented in previous sections of this paper have been analyzed primarily for information on temperature structure evolution, rather than for wind structure evolution. Wind structure evolution is, in general, much more variable than temperature structure evolution. Nevertheless, some important relationships between wind and temperature structures are apparent in the data. The description of the wind systems which follows relies primarily on observations taken in the Eagle Valley where tethered balloon data taken on vertical profiles from the valley floor were supplemented by slope and upper air wind observations.

In the valleys studied, nighttime winds blow down the valleys. The speed of these down-valley flows varies greatly from valley to valley. After sunrise, upslope winds develop in CBLs that grow over the side-walls, and up-floor[1] winds develop in the CBL that grows over the valley floor. The down-valley winds that were present at sunrise within the valley inversion persist in the elevated remnants of the nocturnal inversion layer, hereafter called the "stable core" of the valley atmosphere, during the inversion destruction period. The neutral layer above the stable core appears to be a convective boundary layer that forms over the inclined mesoscale western slope of the Rocky Mountains, i.e., a CBL which forms over the elevated terrain into which the valley has been eroded. The potential temperature of this layer increases with time during the inversion breakup period (see Table 2, column 13 for typical values of warming). Winds in this layer tend to blow up the inclined western slope of the Rockies, but winds in the lower part of the layer may be channeled along the axis of the valley, especially late in the inversion breakup period when the base of the neutral layer has extended downward into the valley. At the top of the neutral layer is the boundary between the neutral layer and the overlying free atmosphere. Winds in the free atmosphere are forced by pressure gradients on a scale extending beyond the mountainous area and are relatively unaffected by the topography below.

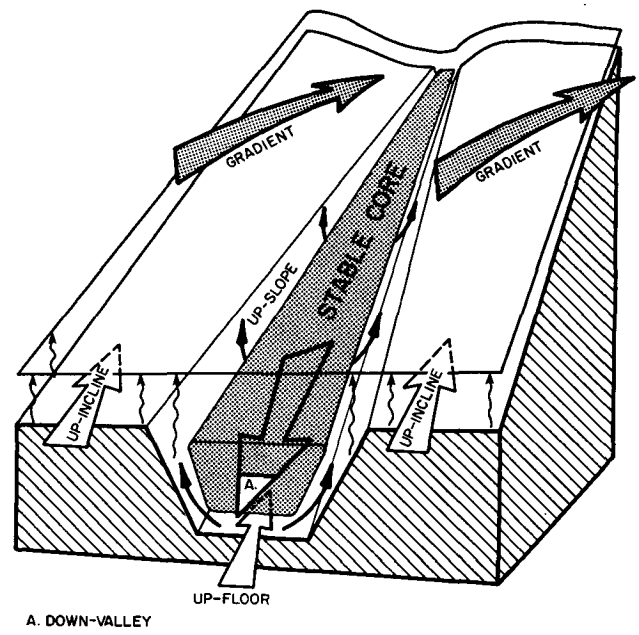

FIG. 8. Typical wind system development at mid-morning during valley inversion breakup.

The dynamic, or changing, nature of the developing wind systems is to be emphasized. After sunrise, convective boundary layers grow upward from sunlit topographic surfaces. The CBLs form over the inclined slopes of the mountain range, the valley sidewalls and the valley floor. The volume of the stable core, containing down-valley winds, continuously decreases from sunrise until inversion destruction. Once the stable core is destroyed, a deep CBL will be present over all the mountain and valley terrain, and the individual up-floor, up-valley and up-slope flows are difficult to differentiate. At a time midway through the inversion breakup cycle the typical wind system patterns are as shown in Fig. 8.

Fig. 9 shows idealized temperature structure-wind system relationships for this same time in terms of vertical soundings taken from the valley floor. Not shown in the figure is the up-slope wind system that

[1] The wind system terminology in this paper emphasizes the essentially bi-directional nature of the local wind systems and their relationship to the underlying terrain features. An "up-floor wind" blows up the valley floor toward the head of a valley in a shallow layer above the floor. This wind may be analogous to the daytime component of Wagner's (1938) "slope wind along the valley floor". An "up-incline wind" blows up the inclined western slope of the Rocky Mountains. The terms "up- and down-valley winds" and "up- and down-slope winds" have their usual meanings.

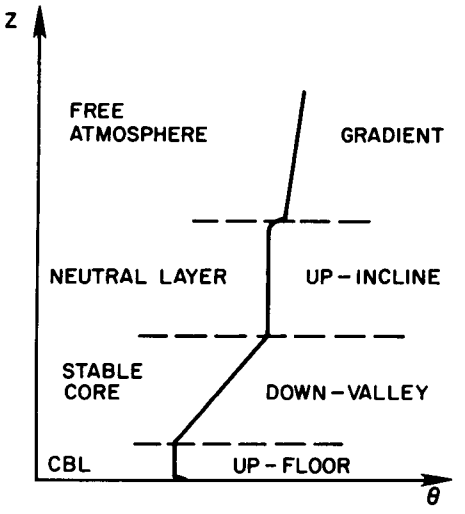

FIG. 9. Typical correspondence between temperature and wind structure during valley inversion breakup.

develops within CBLs that form over the valley sidewalls.

The slow upward growth of the along-floor wind system, the persistence of the down-valley flow in the middle reaches of the valley, and the development and descent into the valley of the up-incline wind system are all features of wind system evolution in Colorado valleys that were not anticipated in early conceptual models of wind system evolution (Wagner, 1938; Defant, 1951) in ideal valleys. The well-mixed neutral layer, in which up-incline winds prevail, is a particularly intriguing observation. Additionally, the observations of the four local wind systems provide a picture of valley wind system evolution that is considerably more complicated than generally expected. These initial observations point out several significant features of valley wind systems. First, with weak upper level winds, the local valley wind systems are forced thermodynamically rather than being forced by momentum transport from aloft. Second, sounding data indicate that the simple concept of winds shifting to up-valley through the valley depth shortly after sunrise is erroneous in the valleys investigated. Wind observations from anemometers on the valley floor would have supported this erroneous view, since winds in the shallow CBL that develops over the valley floor reverse to up-valley shortly after direct sunlight reaches the floor. Finally, the four wind systems are similar in that they develop in boundary layers that form over inclined topographic surfaces.

The reader is referred to the paper by Whiteman (1980) for further details about the local wind systems. Some features of the individual wind systems will be discussed further by referring to data collected in the experimental program. Three experiments were conducted with dual-tethered balloon systems in which observations were collected concurrently from a mid-valley and mid-sidewall site. The observations showed that the top of the temperature inversion was nearly horizontal in the cross-valley section. Upslope wind systems developed over the sidewalls within convective boundary layers after sunrise. Upslope flows on the south-facing slope of the Eagle Valley attained maximum observed depths of 140 m and up-valley wind components attained maximum velocities of 3 m s^{-1}. Wind and temperature structure tended to be unsteady or time-variant within these boundary layers. The descent of the top of the inversion could be seen from the sidewall profiles.

A time-height cross section analysis of along-valley wind components on 13 October 1977 is presented in Fig. 10a as an example of the along-valley wind structure evolution during inversion destruction. At the experimental site, strong down-valley winds usually prevailed in the mid-levels of the valley all night with occasional lulls in wind speeds. On 13 October an apparent lull occurred around 0600 MST. The data illustrate several of the features previously described, including the upward growth from the valley floor after sunrise of the up-floor wind regime, the descent into the valley of channeled up-incline winds, and the persistence of down-valley winds in the stable core during inversion destruction. The persistence of down-valley winds in the stable core for 3 or 4 h after sunrise is a usual feature of the meteorology of this valley. The strength of the down-valley flow, however, usually decreases steadily during this time until, when the stable core becomes thin, a wind reversal occurs and up-valley winds increase in strength. The down-valley flow within the stable core is somewhat steadier than indicated in Fig. 10a, since wind data from both up- and down-soundings are contoured. Fig. 10b is presented for completeness, showing the time- and height-variant cross-valley wind components on the same day.

Due to the limited vertical range of the tethered-balloon data collection systems, it was necessary to use upper-air sounding equipment to investigate the vertical structure of the neutral layer. The analysis of neutral-layer structure must be considered preliminary, given the small number of such observations available. Observations of neutral-layer development are given in Fig. 11, which combines three observations taken on the morning of 14 October 1978 with a single observation taken in the late afternoon of the previous day. No major air mass changes occurred during the two days, and cloud cover was similar, so the four soundings may be considered representative of the evolution of the valley and mountain atmospheric structure on a single day.

The first sounding of the morning, taken shortly after sunrise, shows a strong inversion extending from the surface to about ridgetop level. A 300 m

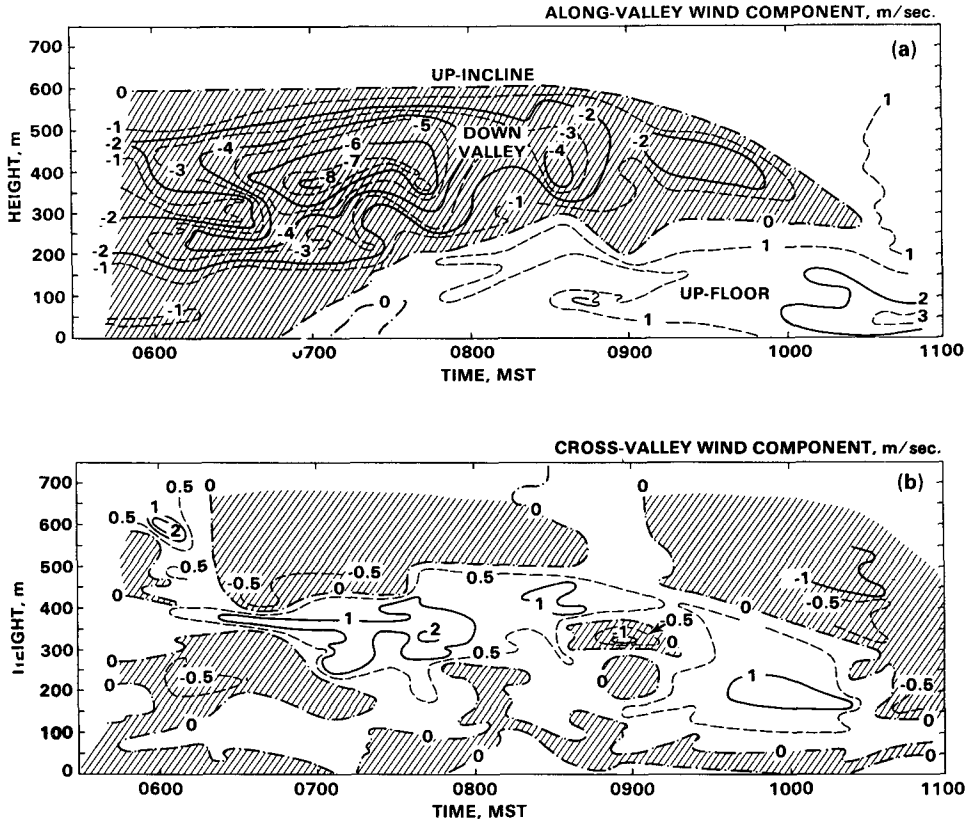

FIG. 10. Time-height analysis of (a) along-valley wind components and (b) cross-valley wind components (both m s^{-1}) as determined from tethered balloon profiles taken from the floor of the Eagle Valley on 13 October 1977. Positive along-valley components blow up the valley. Positive cross-valley components blow from right to left when looking up the valley.

deep isothermal transition layer is present between ridgetop level and the 3100 m MSL base of a neutral layer. The neutral-layer base is at about the level of the general topography surrounding the valley. The top of the neutral layer is capped by a strong stability layer that grades into the free atmosphere above. The evolution of the individual temperature structure layers is apparent in the figure and, except for a transition layer, occurs as described above. The temperature structure layers are closely related to wind structure layers, as shown in the figure.

Some important conclusions can be drawn from this set of data by focusing on the neutral-layer growth. One interpretation of the data is as follows. After sunrise, surface heat flux from the elevated western slopes of the Rockies causes a CBL containing up-incline winds to form over it. Heat flux from the valley surfaces, however, is used to destroy the powerful valley inversion. Only when the valley inversion is destroyed can the valley atmosphere become fully coupled with the CBL that has grown above it. At this time the CBL's over the valley floor and sidewalls, and the stable core (and the transition layer noted in the figure) are no longer distinguishable as separate layers, and the valley atmosphere and the mountain atmosphere above merge into a single CBL containing up-incline winds. These winds may be channeled into the valleys as up-valley winds. An important conclusion, given this scenario, is that the coupling of the valley atmosphere to the free atmosphere involves the development of an intermediate layer.

7. Hypothesis

Warming of the valley atmosphere occurs in one of three ways, as previously described for the three inversion structure evolution patterns. For Pattern 1 inversion destruction over a plain an inversion is broken as a CBL grows upward from the ground. The increase in depth of the CBL and the increasing potential temperature within it come from turbulent sensible heat flux convergence and entrainment of mass into the layer at its top through the action of penetrative convective plumes (Ball, 1960; Stull, 1973). The energy available for sensible heat flux depends on solar heat flux and the partitioning of energy in the surface energy budget. The normal

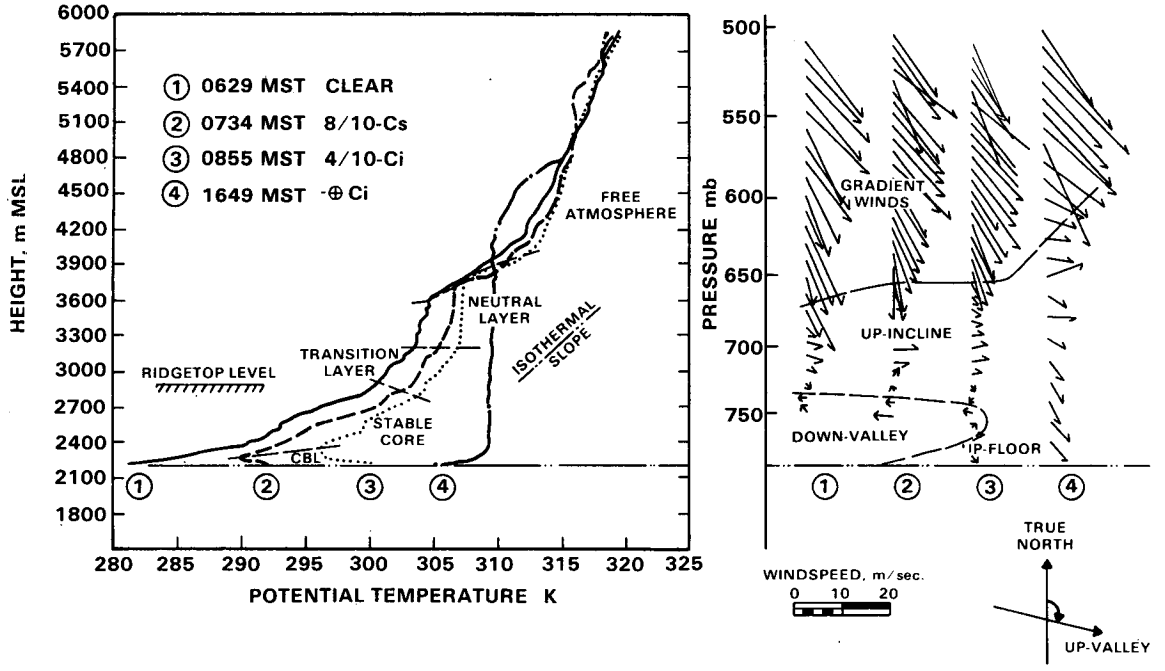

FIG. 11. Upper air soundings taken from the floor of the Eagle Valley during October 1978. Soundings 1–3 were taken on October 14; sounding 4 was taken on October 13. Layers of temperature and wind structure are identified.

growth of the CBL can be retarded by divergence of mass from the CBL or, equivalently, subsidence at its top (Lilly, 1968; Tennekes, 1973). In the case of inversion breakup in a deep valley following Patterns 2 and 3, the warming of the valley atmosphere is accomplished predominantly within the valley inversion layer rather than in the CBL. The warming rate can be approximated by $\partial\theta/\partial t = -w\partial\theta/\partial z$ where w is a negative number on the order of several centimeters per second, and the warming occurs in a layer of the vertical profiles where $\partial\theta/\partial z$ does not change significantly with time. These observations suggest that warming of the deep valley atmosphere occurs predominantly through subsidence. The observations therefore provide an independent, but indirect, verification of the sinking motions over the valley center postulated by prior valley wind theories (Wagner, 1938; Defant, 1951). A prior indirect confirmation of these motions was provided by Hindman (1973) from observations of the breakup of a stratus cloud deck in a California valley. Other investigators, in the absence of direct or indirect measurements of these sinking motions, have doubted their existence in specific valleys [e.g., Buettner and Thyer (1966) in the valleys of Mount Rainier, Washington, and Urfer-Henneberger (1964) for the Dischma Valley of Switzerland].

In the case of Pattern 2 and 3 inversion structure evolution the growth of the CBL is retarded relative to CBL growth over the plains (this is most easily seen in the case of Pattern 2 evolution where the CBL fails to grow after reaching a certain height) and the warming of the CBL is slowed. If the reasonable assumption is made that the energy budgets over the valley floor and plains surfaces are similar and that the surface sensible heat flux provides the energy which warms the valley atmosphere, it is necessary to explain why the valley floor CBL does not warm faster than the CBL over the plains. After all, a shallower layer is expected to warm more rapidly than a deeper layer, given the same energy input. The explanation for this discrepancy is, of course, related to the valley topography which causes the energy to be utilized in a fundamentally different way to produce temperature changes in the valley atmosphere. Over the plains the energy is used to deepen and warm a convective boundary layer. In a valley, as is shown schematically in Fig. 12, the energy may be used to deepen and warm CBLs, but it may also drive the slope flows that carry mass up the sidewalls. Sensible heat flux from valley surfaces causes a convective boundary layer to develop over the valley floor and sidewalls. As over the plains, mass and heat are entrained into these boundary layers from the stable core above. Convergence of heat into the boundary layers warms the air mass within them, causing an upslope flow to develop within the boundary layers over the sidewalls. The divergence of mass from the valley inversion in the upslope flows requires energy, since parcels can be carried up the slope only if they are warmed to the potential temperature of the top of the inversion. From the prin-

ciple of mass continuity and the assumption of no mass convergence or divergence in the along-valley direction, as mass is removed from the base of the stable core and carried away in the upslope flows, the stable core must sink. The evolution of the temperature structure within the valley is thus characterized by the development of convective boundary layers above the valley surface, and sinking or downward advection of the potential temperature structure in the stable core.

This hypothesis can explain many of the observed structural features of the valley atmosphere. The dependence on insolation explains why inversion destruction begins at sunrise. Following the hypothesis, the morning temperature inversion represents an energy deficit that is overcome by continued input of energy into the valley atmosphere. When the valley is snow covered or wet, the available energy is reduced by high albedos or high latent heat. The hypothesis explains the role of the CBLs that have been observed to develop over the valley floor and sidewalls and attributes their retarded growth to divergence of mass from them, or, equivalently, to the strong subsidence field superimposed on them. The hypothesis also explains why the whole depth of the stable core warms at the same rate while the temperature gradient remains constant. The sinking of the stable core can be explained on the basis of the mass continuity equation, where a slow sinking of the broad stable core compensates for stronger rising motions in the shallow boundary layers at its sides. Due to the sinking motion in the stable core, the available energy is utilized to warm the entire valley atmosphere rather than to warm only a boundary layer near the surfaces. Once the valley inversion is destroyed, any further sensible heat flux from the valley surfaces supports the growth of a larger CBL over the entire mountainous region.

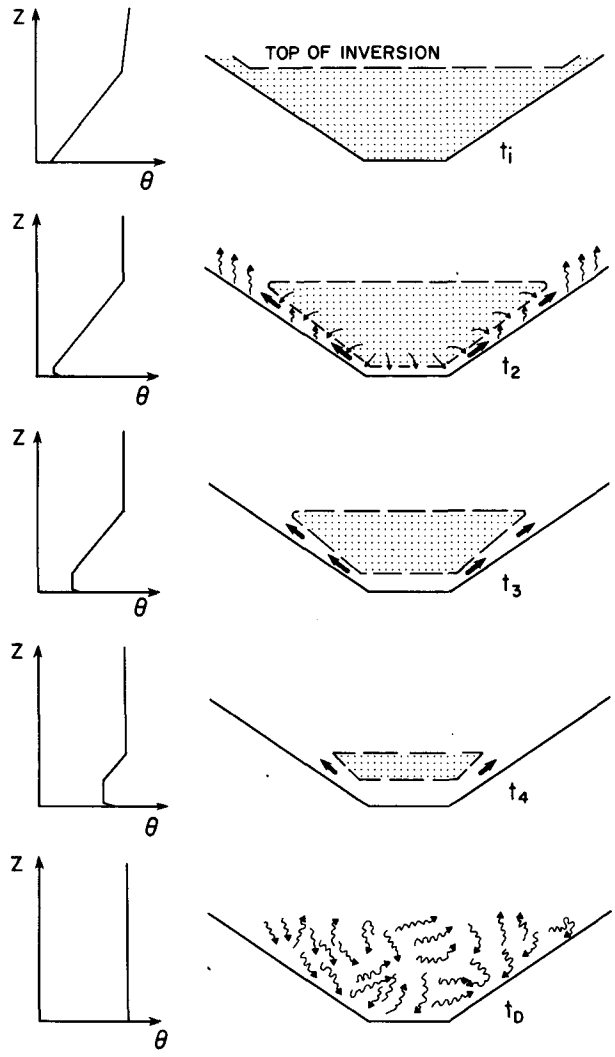

FIG. 12. Illustration of the hypothesis of inversion destruction. On the right side of the diagram cross sections of a valley are shown at times t_i, t_2, t_3, t_4 and t_D. On the left are corresponding potential temperature profiles as taken from the valley center. At sunrise (t_i) an inversion is present in the valley. At t_2, a time after sunlight has illuminated the valley floor and slopes, a growing CBL is present over the valley surfaces. Mass and heat are entrained into the CBLs from the stable core above and carried up the sidewalls in the upslope flows. This results in a sinking of the stable core and growth of the CBLs (t_3 and t_4) until the inversion is broken (t_D) and a turbulent well-mixed, neutral atmosphere prevails through the valley depth.

8. Summary and conclusions

An extensive observational program was conducted in valleys of western Colorado to determine how the temperature structure of the valley atmosphere evolves following sunrise during the time when the nocturnal surface-based radiation inversions are destroyed. Experiments were conducted mainly in clear, undisturbed weather in valleys of varied topography. A tethered balloon sounding system was used to collect temperature, humidity, pressure, wind speed and wind direction data.

At sunrise nocturnal inversions in most of the valleys were built up to about the level of the surrounding ridgetops. The average depth, based on 21 case studies, was 604 m. Vertical potential temperature gradients within the inversions averaged 0.0295 K m^{-1}, but ranged from 0.0187 to 0.0566 K m^{-1}. The strength and direction of prevailing winds aloft, as determined from the Grand Junction, Colorado morning rawinsonde sounding, had no demonstrable effect on the characteristics of valley inversions and the valley inversions showed much less variability from day to day and season to season than inversions over Grand Junction. This suggests that, at least for a narrow range of synoptic conditions, valley topography produces more consistent inversions, perhaps by protecting them from the winds aloft.

When the along-valley winds were weak, the valley

vertical potential temperature profiles frequently were hyperbolic, especially near the ground. In most valleys where along-valley winds were of at least moderate strength, the inversion profiles were nearly linear with height.

Temperature inversions in all of the valleys investigated were destroyed after sunrise following one of three patterns of temperature structure evolution. The first pattern, observed in the widest valley studied, approximates inversion destruction over flat terrain, in which the nocturnal inversion is destroyed after sunrise by the upward growth from the ground of a warming convective boundary layer. The second pattern, observed in snow-covered valleys, differs significantly from the first. Here the growth of the CBL, which begins after sunrise, is arrested once the CBL has attained a depth of 25–50 m. The inversion is then destroyed as the top of the nocturnal inversion descends into the valley. Successive profiles of the valley atmosphere show a warming consistent with a simple subsidence of the previous profiles. The third pattern of temperature structure evolution, being a more general case of the first and second patterns, was observed in all the valleys when snow cover was not present and describes the majority of case studies observed in field experiments. Following this pattern, inversions are destroyed by two processes: the continuous upward growth from the valley floor of a warming CBL and the continuous descent of the top of the nocturnal temperature inversion. Warming of the elevated inversion layer above the CBL is consistent with a simple subsidence of the previous profiles. In the Colorado valleys studied, the time required to break an inversion and establish a neutral atmosphere within the valley was typically 3½–5 hours after sunrise. Temperature structure evolution during clear, undisturbed weather was surprisingly uniform from day to day and season to season. Thus, in future work, one may be fairly confident of observing typical inversion breakup during short field studies in undisturbed weather.

The common element of all three patterns of temperature structure evolution is the development of a CBL over the valley floor after it is illuminated by direct sunlight. Observations taken from the sidewall of one valley also show the development of a CBL after direct sunlight illuminates the sidewall. Due to the shading effects of surrounding topography, the different valley surfaces can be illuminated at significantly different times, thus affecting the initiation of CBL growth. The temperature structure of the sidewall CBL is similar to that of the CBL over the valley floor, but winds blow up the sidewall CBL at speeds of up to 3 m s^{-1}.

Five different temperature structure layers have been observed during the inversion destruction period. Above the valley floor CBL and the sidewall CBL just mentioned is the stable core of the potential temperature inversion. A neutral stability layer above the stable core appears to be part of a larger scale convective boundary layer that forms over the Western Slope of the Rocky Mountains. Above this layer is the free atmosphere, characterized by a more stable temperature structure.

Each of the five temperature structure layers, while identified primarily by their potential temperature structure, can also be identified by the winds that prevail within them. During inversion destruction, the CBLs over the valley floor and sidewalls contain winds which blow up the floor of the valley and up the slopes. The CBL, or neutral layer, above the valley inversion has winds which blow up the inclined Western Slope of the Rocky Mountains during the day. Winds in the stable core typically continue to blow down-valley after sunrise until the stable core is nearly destroyed. Winds in the stable free atmosphere may blow from any direction with speeds determined by synoptic-scale pressure gradients. A great variability was observed from day to day and from valley to valley in the wind structure within the free atmosphere, the neutral layer, the stable core, and the valley floor CBL. Despite this variability in the strength and timing of reversal of the winds, the temperature structure evolved uniformly from day to day.

On the basis of the wind and temperature observations summarized above, an hypothesis has been developed to explain the temperature structure evolution. Since energy is required to change the temperature structure, and the changes begin at sunrise, it is reasonable to hypothesize that solar radiation is the driving force. A fraction of the solar radiation, received on the valley floor and sidewalls, is converted to the sensible heat flux that provides energy to the valley atmosphere. Sensible heat flux from a surface, as over flat terrain, causes a convective boundary layer to develop over the surface. Mass and heat are entrained into the CBL from the stable core above. Mass entrained into the valley floor and sidewall CBLs, however, is carried from the valley in the upslope flows that develop in the convective boundary layers over the sidewalls. This removal of mass from the base and sides of the stable core causes the elevated inversion to sink deeper into the valley and to warm adiabatically due to subsidence, and decreases the rate of growth of the CBLs. Following this hypothesis, the rate of warming depends directly on the rate of energy input into the valley atmosphere. This energy may be used to deepen the CBLs or to move mass up the sidewalls, allowing the stable core to sink.

Acknowledgments. The author wishes to thank Dr. Thomas B. McKee for valuable advice, encouragement and support in all aspects of the work. The Field Observing Facility of the National Center for

Atmospheric Research provided equipment and the valuable services of a field technician, who helped collect much of the data. The author is indebted to many individuals for field and other support, which is greatly appreciated.

The research was accomplished at the Department of Atmospheric Science, Colorado State University, with funding from the Atmospheric Sciences Section, National Science Foundation, under Grant ATM76-84405. The manuscript was prepared with funding from the U.S. Environmental Protection Agency through Interagency Agreement AD-89-F-097-0 with the U.S. Department of Energy.

REFERENCES

Ball, F. K., 1960: Control of inversion height by surface heating. *Quart. J. Roy. Meteor. Soc.*, **86**, 483–494.

Buettner, K. J. K., and N. Thyer, 1966: Valley winds in the Mount Rainier area. *Arch. Meteor. Geophys. Bioklim.*, **B14**, 125–147.

Davidson, B., and P. K. Rao, 1963: Experimental studies of the valley-plain wind. *Int. J. Air Water Pollut.*, **7**, 907–923.

Defant, F., 1951: Local Winds. *Compendium of Meteorology*, T. M. Malone, Ed. Amer. Meteor. Soc., 655–672.

Ekhart, E., 1949: Über Inversionen in den Alpen. *Meteor. Rund.*, **2**, 153–159.

Geiger, R., 1965: *The Climate Near the Ground*, rev. ed. Harvard University Press, 611 pp. [Translated by Scripta Technica, Inc. from the 4th German edition, 1961.]

Hindman, E. E., II, 1973: Air currents in a mountain valley deduced from the breakup of a stratus deck. *Mon. Wea. Rev.*, **101**, 195–200.

Lilly, D. K., 1968: Models of cloud-topped mixed layers under a strong inversion. *Quart. J. Roy. Meteor. Soc.*, **94**, 292–309.

Machalek, A., 1974: Inversionsuntersuchungen in einem Gebirgstal. *Wetter und Leben*, **26**, 157–168.

Morris, A. L., D. B. Call and R. B. McBeth, 1975: A small tethered balloon sounding system. *Bull. Amer. Meteor. Soc.*, **56**, 964–969.

Reid, J. D., 1976: Dispersion in a mountain environment. Atmos. Sci. Pap. No. 253, Colorado State University, 150 pp.

Scorer, R. S., 1973: *Pollution in the Air-Problems, Policies and Priorities*. Routledge and Kegan Paul Ltd., 148 pp.

Sellers, W. D., 1965: *Physical Climatology*. The University of Chicago Press, 272 pp.

Stull, R. B., 1973: Inversion rise model based on penetrative convection. *J. Atmos. Sci.*, **30**, 1092–1099.

Tennekes, H., 1973: A model of the dynamics of the inversion above a convective boundary layer. *J. Atmos. Sci.*, **30**, 558–567.

Urfer-Henneberger, 1964: Wind- und Temperaturverhältnisse an ungestörten Schönwettertagen im Dischmatal bei Davos. *Mitt. Schweiz. Anst. Forstl. Versuchsw.*, **40**, 389–441.

Wagner, A., 1938: Theorie und Beobachtung der periodischen Gebirgswinde. *Gerlands Beitr. Geophys.*, **52**, 408–449.

Whiteman, C. D., 1980: Breakup of temperature inversions in Colorado mountain valleys. Ph.D. dissertation, Colorado State University, 256 pp.; also Atmos. Sci. Pap. No. 328, Colorado State University.

——, and T. B. McKee, 1977: Observations of vertical atmospheric structure in a deep mountain valley. *Arch. Meteor. Geophys. Bioklim.*, **A26**, 39–50.

——, and ——, 1982: Breakup of temperature inversions in deep mountain valleys: Part II. Thermodynamic model. *J. Appl. Meteor.*, **21**, 290–302.